Cellular/Molecular

Caenorhabditis elegans Innexins Regulate Active Zone Differentiation

Edward Yeh,[1]* Taizo Kawano,[1]* Sharon Ng,[1,2]* Richard Fetter,[3] Wesley Hung,[1] Ying Wang,[1] and Mei Zhen[1,2]

[1]Samuel Lunenfeld Research Institute, Montana Sinai Hospital, Toronto, Ontario M5G 1X5, Canada, [2]Department of Molecular Genetics, University of Toronto, Toronto, Ontario M5S 1A8, Canada, and [3]Howard Hughes Medical Institute, The Rockefeller University, New York, New York 10021

In a genetic screen for active zone defective mutants in *Caenorhabditis elegans*, we isolated a loss-of-function allele of *unc-7*, a gene encoding an innexin/pannexin family gap junction protein. Innexin UNC-7 regulates the size and distribution of active zones at *C. elegans* neuromuscular junctions. Loss-of-function mutations in another innexin, UNC-9, cause similar active zone defects as *unc-7* mutants. In addition to presumptive gap junction localizations, both UNC-7 and UNC-9 are also localized perisynaptically throughout development and required in presynaptic neurons to regulate active zone differentiation. Our mosaic analyses, electron microscopy, as well as expression studies suggest a novel and likely nonjunctional role of specific innexins in active zone differentiation in addition to gap junction formations.

Introduction

Synaptic vesicles release neurotransmitters at electron dense presynaptic plasma membrane regions generally termed as active zones (Couteaux and Pecot-Dechavassine, 1970; Zhai and Bellen, 2004). To elucidate mechanisms that regulate active zone formation, we developed fluorescent active zone markers in *C. elegans* and identified a number of mutations affecting their expression patterns. Some mutations do not significantly alter synaptic vesicle markers, making them the ideal candidates for specific regulators of active zones (Yeh et al., 2005). Here, we report the identification of two such candidates, innexins UNC-7, and UNC-9.

Innexins, connexins, and pannexins are components of gap junctions, the intercellular channels that allow for the exchange of ions and other small signal molecules (Kumar and Gilula, 1996). Gap junctions are consisted of two hemichannels residing on apposing membranes of adjacent cells. Ultrastructually, they appear as electron dense regions joining apposing plasma membranes 3–5 nm apart (Revel and Karnovsky, 1967). Gap junctions mediate the electrical coupling, which synchronizes neuronal activities and influences the development of neural circuits (Personius and Balice-Gordon, 2002; Bennett and Zukin, 2004; Hestrin and Galarreta, 2005). Gap junctions also play an essential role in the propagation of calcium for long-range signaling by glial cells (Venance et al., 1997; Höfer et al., 2002).

Connexins and pannexins are the two mammalian families of gap junction proteins that share no sequence homology but similar predicted topology (Bruzzone et al., 2003). The roles of connexins in forming gap junctions are well documented (Connors and Long, 2004; Söhl et al., 2005). The *in vivo* functions of pannexins, however, are poorly understood despite of their abundant neuronal expression (Vogt et al., 2005; Dvoriantchikova et al., 2006). Exogenously expressed Pannexin-1 forms gap junctions and also functions as hemichannels (Bruzzone et al., 2003; Locovei et al., 2006; Vanden Abeele et al., 2006). Some endogenous Pannexin-1 localizes postsynaptically in rodent neurons in a nonjunctional manner (Zoidl et al., 2007); furthermore, they contribute to the hemichannel activities under ischemic conditions and epileptiform seizure activity in neurons (Thompson et al., 2006). This, together with other studies (Pelegrin and Surprenant, 2006; Romanov et al., 2007) implicate that Pannexin-1 may also have a nonjunctional role *in vivo*.

Most invertebrates contain only innexins (Landesman et al., 1999; Phelan and Starich, 2001). Among the 25 innexins in *C. elegans* and eight in *Drosophila*, only a few have been characterized (Watanabe and Kankel, 1990; Krishnan et al., 1993; Phelan et al., 2008). In *C. elegans*, different innexins have been implicated in electrical coupling between pharyngeal muscles (Li et al., 2003), gap junction-mediated oocyte maturation (Whitten and Miller, 2007), sensory neuron identity (Chuang et al., 2007), and calcium propagation in the gut (Peters et al., 2007). Innexins UNC-7 and UNC-9 were first isolated through their requirement for coordinated locomotion (Starich et al., 1993; Barnes and Hekimi, 1997), but the origin of the locomotion deficit remains unknown. Although UNC-9 mediates the electrical coupling between body-wall muscles (Liu et al., 2006), the lack of this activity contributes little to the locomotion defects (Chen et al., 2007; our unpublished observation).

Received Feb. 6, 2009; revised March 13, 2009; accepted March 16, 2009.

This work was supported by Canadian Institute of Health Research Grants (MOP-74530 and GMH-79044) awarded to M.Z. We thank D. Hall, D. Holmyard, R. Temkin, and K. Schuske for assistance in preparing EM samples; E. Liao, C. Jiang, and C. Hwang for help generating *hpIs54* marker; B. Bamber, Y. Jin, and M. Nonet for *oxIs22*, *juIs1*, and *jsIs129* markers, respectively; T. Starich and J. Shaw for sharing anti-UNC-7 antibody, *lwIs48*, and *unc-9(fc16) dyf-6 unc-7(e5)* strains prior to publication; we also thank T. Starich and J. Shaw for sharing unpublished results and discussions; Z. Wang for rabbit sera against UNC-9; M. Nonet for UNC-10 antibodies; A. Coulson for *C. elegans* genomic DNA cosmids; M. Vidal for a *C. elegans* cDNA library; J. Culotti for the *unc-129* promoter; and *C. elegans* Center for various strains. We are grateful for comments from C. Bargmann and T. Starich on this manuscript.

*E.Y., T.K., and S.N. contributed equally to this work.

Correspondence should be addressed to Mei Zhen, Samuel Lunenfeld Research Institute, Montana Sinai Hospital, Toronto, ON M5G 1X5, Canada. E-mail: zhen@mshri.on.ca.

R. Fetter's present address: Electron Microscopy Shared Resource, Howard Hughes Medical Institute/Janelia Farm Research Campus, 19700 Helix Drive, Ashburn, VA 20147.

DOI:10.1523/JNEUROSCI.0637-09.2009

 0270-6474/09/295207-11$15.00/0

Recent studies revealed novel roles for connexins to mediate cell migration independent of channel activities (Xu et al., 2006; Elias et al., 2007). We propose here another novel role of two *C. elegans* innexins in active zone differentiation, likely through a gap-junction independent mechanism.

Materials and Methods

Strains and constructs. Standard methods were used for culturing and handling animals (Brenner, 1974). For details of strains and constructs generated and used, see supplemental Materials, available at www.jneurosci.org.

Cloning of hp121. *hpIs3(Punc-25*-GFP::SYD-2)*hp121* mutants were outcrossed four times against N2. The GFP::SYD-2(*hpIs3*) phenotype was followed in each outcross and the *unc* (*unc*oordinated locomotion) phenotype always associated with the GFP::SYD-2(*hpIs3*) marker defects. GFP::SYD-2(*hpIs3*) phenotype was used for genetic mapping to place it to the right arm of chromosome X. Fine mapping was performed using the *unc* phenotype, followed by confirmation of the GFP::SYD-2(*hpIs3*) defects to place it close to the same locus as *unc-7*. We conclude *hp121* encodes *unc-7* by (1) complementation tests against *hpIs3unc-7(e5)* (supplemental Materials, available at www.jneurosci.org), and *hpIs3unc-7(hs9)* (using males generated at the permissive temperature) showed that *hp121* failed to complement both alleles of *unc-7* in regards to both *unc* and GFP::SYD-2 phenotypes; (2) a clone that harbors only the genomic region of *unc-7* (pJH371) (supplemental Materials, available at www.jneurosci.org) fully rescued the *unc* and GFP::SYD-2 defects of *hp121hpIs3* animals; (3) sequencing of the *unc-7* cDNA isolated from *hpIs3hp121* mutants revealed a G to A change that leads to an early stop codon at W192 (TGG to TGA); (4) *hp121hpIs3* animals display no immunofluorescent signals when stained by antibodies against UNC-7.

Immunocytochemistry. Animals were fixed in 2% paraformaldehyde for 2 h and processed as described previously (Zhen and Jin, 1999). Under these conditions, green fluorescent protein (GFP) fusion proteins are preserved and visualized and imaged directly. An exception is in Figure 4, where a mouse monoclonal antibody against GFP (Roche) and rabbit polyclonal antibody against monomeric red fluorescent protein (mRFP) (Clontech) were used to detect the fusion proteins. Antibodies against UNC-7 were generated against the C-terminal 88 aa (S435-D522) of UNC-7 in rabbit (a gift from Drs. T. Starich and J. Shaw, University of Minnesota, Minneapolis, MN) (T. Starich, J. Xu, M. Skerrett, B. Nicholson, and J. Shaw, unpublished observations). The UNC-9-specific antibody was purified from the crude rabbit antisera (Chen et al., 2007) against the last 77 aa of UNC-9. Antibodies against UNC-7, UNC-9, UNC-10 (Koushika et al., 2001), SYD-2 (Yeh et al., 2005), GFP, and mRFP were used at 1:50, 1:100, 1:200, 1:12,000, 1:200, 1:200, and 1:200 dilution, respectively. Alexa Fluor 488 and 594 conjugated donkey anti-rabbit, donkey anti-rat, and donkey anti-chicken (Invitrogen) secondary antibodies were used at 1:400 dilution.

Imaging and quantification of puncta. Quantification of fluorescent markers GFP::SYD-2(*hpIs3*) and Synaptobrevin::GFP(*juIs1*) was performed as described previously with modification (Yeh et al., 2005). Briefly, the quantification of *hpIs3* (GFP::SYD-2) puncta was performed by two methods: (1) a visual examination and counting of fluorescent puncta in the specific region as described; (2) pictures of the marker expression in the same region with the same setting on a charge-coupled device camera and the number of puncta counted from the pictures. For this study, we used a setting of the camera that gives similar puncta number as by live visual examination for wild-type animals. Quantification of the fluorescent marker *hpIs61* (*Punc*-25-UNC-10::GFP) was performed by taking pictures of the defined regions under the same sitting and the pictures automatically analyzed by an in-house developed Matlab program called Punctaanalyzer and R script (Hung et al., 2007; Kim et al., 2008). For all analyses, the examiners were blinded for the genotype of the animals. All supplemental Movies, available at www.jneurosci.org as supplemental material, were captured on a Zeiss Stemi SVII dissecting microscope equipped with a Zeiss Axiocam digital camera.

Aldicarb assays. Nematode growth medium (NGM) plates were supplemented with 1 mM of aldicarb diluted from a 100 mM stock made fresh in acetone. Aldicarb plates were prepared 1 d before the assay. Paralysis was scored every 20 min for the duration of 2 h. *unc-10(md1117)* animals were used as positive controls. Paralysis was defined as the lack of forward or backward movement with a straight body posture and rigidity. All strains shown on a single graph were assayed together. The graphs shown in Figure 3*A* is a representative set of results. Each experiment was repeated more than five times.

Electron microscopy. For active zone analyses in adults, samples were processed and fixed by high-pressure freezing as described previously (Rostaing et al., 2004) with slight modification (Wang et al., 2006), and 70 nm serial sections were collected. Images of nerve cords were collected on a Tecnai20 electron microscope equipped with a Gatan Dualview digital camera. Individual GABAergic and cholinergic motoneurons were traced and reconstructed over at least 150 serial sections in each sample [two wild-type animals with 11 GABAergic neuromuscular junctions (NMJs) and 22 cholinergic NMJs; and 2 *unc-7(hp121)* animals, 27 GABAergic NMJs and 41 cholinergic NMJs], to allow unambiguous classification of GABAergic and cholinergic NMJs. GABAergic and cholinergic synapses are distinguished based on their location within the nerve cord and their targeting pattern (White, 1986). NMJs are defined as large varicosities along the processes of A, B, and D classes of motoneurons that quickly emerge while moving out of the ventral or dorsal nerve cords toward the muscle arms and disappear when the processes "dive" back to the nerve cords. In wild-type animals, these varicosities are associated with the appearance of synaptic and dense-core vesicles, cadherin junction-like structures with the muscle arm, and a single active zone that is defined as the electron dense area at the plasma membrane surrounded by synaptic vesicles. The total volume of active zones in a synapse is measured by multiplying the combined surface area of the active zone in all sections of the synapse by 70 nm.

For gap junction analyses in first larval stage (L1) larvae, animals were fixed by high-pressure freezing and processed as described previously (Chuang et al., 2007). Serial sections (50 nm) were collected from one sample for 50 serial sections along the dorsal nerve cord and 40 serial sections along the ventral nerve cord. Five bona-fide gap junctions were identified in the series by the following criteria: (1) juxtaposed junctions with flattened, straightened morphology all the way across the contacting membranes for at least two consecutive sections; (2) increased electron density in the "gap" compared with close apposition of adjacent membranes; (3) the width of the electron density in the gap of 3–5 nm; and (4) the cytoplasmic-to-cytoplasmic distance across the gap $<$20 nm.

Temperature shift assays. Synchronized *C. elegans* embryos were collected from gravid *hpIs3*(*Punc-25*-GFP::SYD-2)*unc-7(hs9)* adults. In all temperature upshift experiments, collected embryos were hatched and maintained at 15°C on NGM plates and shifted to 22°C at the desired developmental stage. Animals were maintained at 22°C until the adult stage for a qualitative examination of the marker phenotype. Downshift experiments were done similarly, except embryos were cultured at 22°C and shifted to 15°C at specific stages. Developmental stages of animals were determined based on the presence/absence of L1 and adult alae and the anatomy of the somatic gonad and vulva as described previously (Sulston and Horvitz, 1977).

Mosaic analysis. pJH621, pJH442, and P*odr-1*::GFP injection marker were coinjected in *hpIs3 unc-7(hp121)* animals to generate *hpEx525*. Transgenic L4-stage animals displaying tdTomato expression in the DD1 cell body but lacking such expression in DD2 (and vice versa) were first identified by fluorescent microscopy in the RFP channel, imaged at the GFP channel, and photographed and analyzed as described previously (Yeh et al., 2005).

Statistical analysis. Averages for pooled data are presented with error bars representing SD. *p* values were calculated using the *t* test function in Microsoft Excel or R-script (Yeh et al., 2005; Kim et al., 2008).

Results

unc-7 is required for the even distribution of GFP::SYD-2 active zone markers

Using a fluorescent active zone marker, *hpIs3* (*Punc-25*-GFP::SYD-2), we performed a forward genetic screen for active

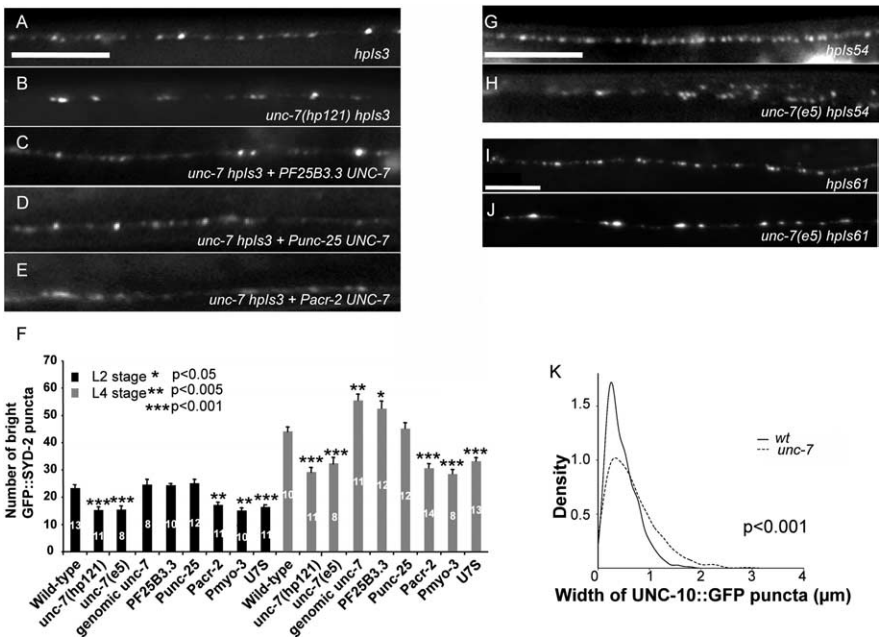

Figure 1. Mutations in *unc-7* specifically affect active zone differentiation. ***A–E***, GABAergic active zone marker *hpIs3* (*Punc-25-GFP*::SYD-2) expression in wild-type (*hpIs3*), *unc-7(hp121)*, *unc-7(hp121)* plus panneuronal *unc-7*, *unc-7(hp121)* plus GABAergic *unc-7* and *unc-7(hp121)* plus Cholinergic *unc-7* L2 stage larvae. ***F***, *unc-7(hp121)* animals carrying a genomic *unc-7* construct, an UNC-7S construct, or constructs that express *unc-7* pan-neuronally (P*F25B3.3*) in muscles (P*myo-3*), in GABAergic (P*unc-25*), or in cholinergic (P*acr-2*) neurons were quantified for the bright GFP::SYD-2 puncta in DD5 motoneurons. The number in each bar graph shows the number of animals analyzed. ***G***, ***H***, Cholinergic active zone marker *hpIs54* (GFP::SYD-2) expression in wild-type (*hpIs54*) and *unc-7*(*e5*) L2 stage larvae. ***I***, ***J***, Another GABAergic active zone marker *hpIs61* (*Punc-25-GFP*::UNC-10) expression in wild-type (*hpIs61*) and *unc-7(e5)* L3 stage larvae. Scale bar, 5 μm. ***K***, The distribution curve of the *hpIs61* punctum width in L3 stage larvae of wild-type (solid line) and *unc-7(e5)* (dotted line) animals. *x*-axis represents the punctum width in micrometers; *y*-axis represents the density or the distribution of puncta in arbitrary units. *N*, The total number of puncta used for analyses: 577 for wild type, 490 for *unc-7*.

zone defective mutants (Yeh et al., 2005) and isolated *hp121*, an allele of a previously identified innexin gene, *unc-7* (Starich et al., 1993). *hp121* harbors a missense mutation that creates an early stop codon in the predicted protein sequence (W192; Materials and Methods). In wild-type L2 animals, GFP::SYD-2 (*hpIs3*) puncta are of even extensity and evenly distributed along the dorsal nerve cord (Fig. 1*A*). In *unc-7(hp121)* mutants, while the total fluorescent punctum number remains similar to that of wild-type animals, fewer bright GFP::SYD-2 (*hpIs3*) puncta were observed along the dorsal cord, displaying regions composed of only dim fluorescent puncta (gaps) (Fig. 1*B*). A qualitative assessment of the GFP::SYD-2 (*hpIs3*) puncta in the DD5 motoneuron (Yeh et al., 2005) showed an ~34% reduction in the number of the bright and countable *hpIs3* puncta throughout development (Fig. 1*F*). A previously identified null allele of *unc-7(e5)* displayed a similar level of reduction in the bright GFP::SYD-2 (*hpIs3*) puncta (Fig. 1*F*). *e5* and *hp121* mutants show no staining with antibodies against UNC-7 (data not shown) and failed to complement each other. In addition to the active zone defects, both *hp121* and *e5* animals display identical uncoordinated (Unc) behavior. Compared with wild-type animals that display smooth, sinusoidal body bends during locomotion, *unc-7* mutant animals move in a rigid and twisted manner referred as "kinkers" [compare supplemental Movie S1 (wild type) with S2 (*hp121*) and S3 (*e5*), available at www.jneurosci.org as supplemental material]. Both the Unc behavior and the reduction of the bright GFP::SYD-2(*hpIs3*) puncta in *hp121* mutants were fully rescued by a DNA fragment containing only the *unc-7* genomic sequences (Fig. 1*F*; supplemental Movie S4, available at www.jneurosci.org as supplemental material). Together, this suggests that *hp121* represents another allele of *unc-7* and mutations in *unc-7* cause defective locomotion and active zone differentiation.

The original active zone screen was performed using a GABAergic active zone marker. We further examined active zone differentiation in other motoneurons using *hpIs54* (P*unc-129*-GFP::SYD-2), a strain that expresses GFP::SYD-2 in DA and DB class cholinergic motoneurons. Wild-type animals express discrete GFP::SYD-2(*hpIs54*) puncta that are uniform in brightness and even distribution along the dorsal cord (Fig. 1*G*). In contrast, *unc-7* mutants showed a disorganized distribution of bright and dim puncta along the dorsal nerve cord (Fig. 1*H*). Therefore, the GFP::SYD-2 active zone markers in both GABAergic and cholinergic synapses are affected in *unc-7* mutant animals, supporting a general role for *unc-7* in active zone differentiation.

unc-7 is specifically required for proper active zone differentiation

To determine whether the reduction observed in GFP::SYD-2 puncta reflects general defects in synaptic differentiation, we examined the expression patterns of other synaptic markers in *unc-7* mutants. *hpIs61*(*Punc-25*-GFP::UNC-10) is another active zone marker that expresses the GFP-tagged active zone scaffolding protein UNC-10 (Koushika et al., 2001; Yeh et al., 2008) in the GABAergic motoneurons. In wild-type larvae expressing the *hpIs61* marker, GFP::UNC-10 puncta of even size and spacing are present along the dorsal cord (Fig. 1*I*). In *unc-7* mutants, there is a very small reduction of the total number of GFP::UNC-10 puncta along the dorsal nerve cord (129.1 ± 3.4, $N = 14$ vs 139.9 ± 6.3, $N = 16$ wild type; $p < 0.0001$). Similar to the GFP::SYD-2 marker, the size and distribution of these GFP::UNC-10 puncta are irregular in *unc-7* mutants (Fig. 1*J*); some GFP::UNC-10 puncta display increased fluorescent intensity and size, whereas others become dim and small, thus appearing as small "gaps" along the nerve processes. We quantified this difference by comparing the distribution curve of the width of GFP::UNC-10 puncta in wild-type and *unc-7(e5)* animals. Unlike in wild-type animals, where a majority of the puncta showed similar width, shown as a shape peak in the Kernel's density curve (Fig. 1*K*, solid line), the punctum width in *unc-7(e5)* mutants was more variable, with increased fractions of large puncta (Fig. 1*K*, dotted line) ($p < 0.001$ vs wild type).

In contrast, *juIs1* (Synaptobrevin::GFP) and *jsIs219* (Synaptogyrin::GFP), two synaptic vesicle markers for the GABAergic motoneurons and the entire nervous system, respectively (Nonet, 1999; Zhen and Jin, 1999), showed normal morphology, as well as normal number and distribution of dorsal or lateral cord puncta in *unc-7* animals (supplemental Fig. S1, available at www.jneurosci.org as supplemental material). Thus, *unc-7* mutations preferentially affect active zone markers, suggesting that UNC-7 innexin has specific roles in active zone morphology or composition. Consistent with a change in the organi-

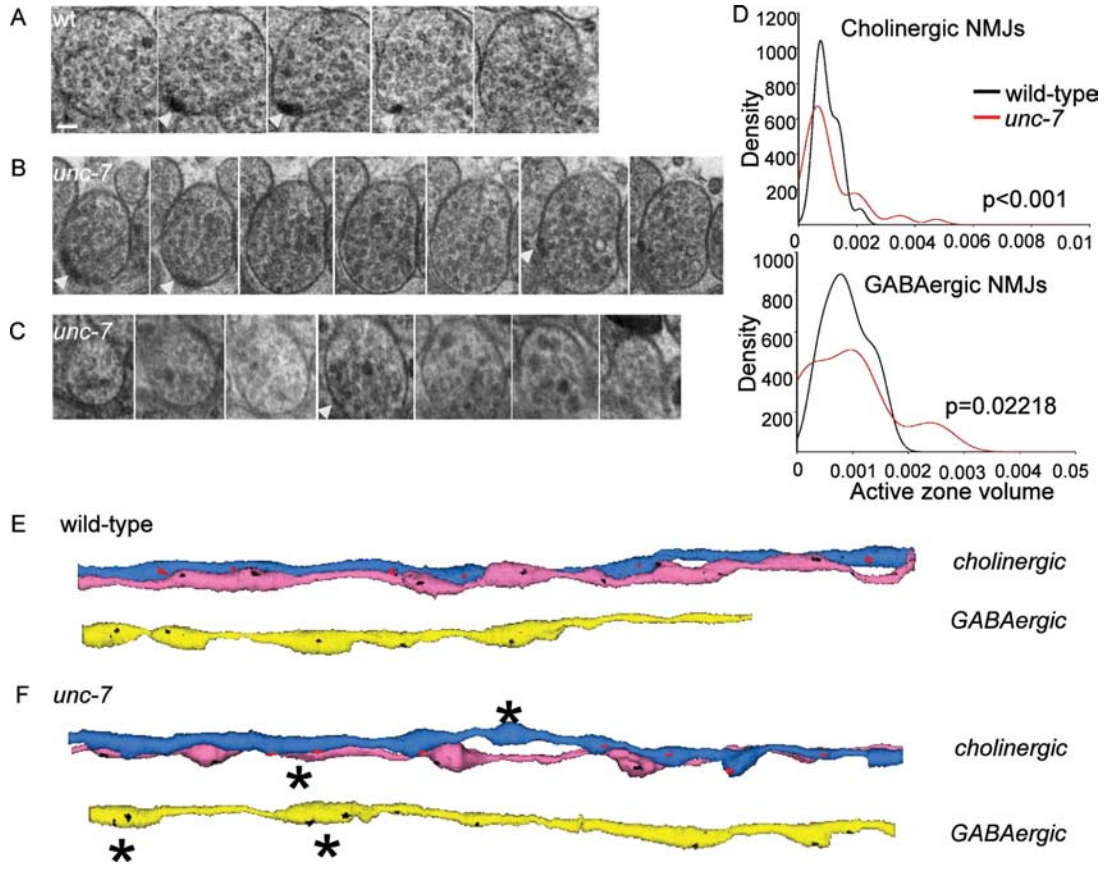

Figure 2. Ultrastructural analysis of the active zone morphology in *unc-7* animals. ***A–C***, Serial electron micrographs of one GABAergic NMJs in wild-type animals (***A*** series) and two GABAergic NMJs in *unc-7* mutants (***B*** and ***C*** series). White arrowheads mark the position of the active zone(s) in each synapse. Active zones in *unc-7* animals can be larger (***B***) or less prominent (***C***). Scale bar, 100 nm. ***D***, The distribution curve of active zone size in wild-type and *unc-7* animals. *x*-axis represents the volume in micrometers cubed; *y*-axis represents the density of active zones in arbitrary units. ***E***, ***F***, Cholinergic and GABAergic nerve processes of a wild-type and a *unc-7* animal reconstructed from serial electron micrographs. The varicosities along the axons are synapses, and the active zone(s) in each synapse are also traced and shown as either black or red dots. Asterisks mark abnormal synapses in *unc-7* neurons with irregular active zones.

zation in active zones, we also observed a small but corresponding change with a postsynaptic receptor marker *oxIs22* (GABA receptor::GFP) with abnormal clustering and distribution in *unc-7* mutants (supplemental Fig. S1*C*, available at www.jneurosci.org as supplemental material).

To examine if the changes we observed with the various synaptic markers reflect actual active zone structural defects, we performed partial serial electron microscopic reconstructions of nerve cords of wild-type and *unc-7(hp121)* adults. Consistent with a previous report [J. White, T. Starich, and J. Shaw, personal communication, cited by Starich et al. (1993)], no global loss of gap junctions was observed in our *unc-7* samples (for example, see Fig. 5*D*). Individual GABAergic and cholinergic motoneurons were traced and reconstructed over at least 100 sections in each sample to allow unambiguous identification of GABAergic and cholinergic NMJs. The active zone is defined as the electron dense region at the plasma membrane surrounded by synaptic vesicles in those NMJs (White, 1986). The active zone volume was calculated by multiplying the total surface area of the active zone in each synapse by the thickness of the section.

In wild-type animals, the majority of GABAergic and cholinergic NMJs contain a single active zone area of similar volume (Fig. 2*A*,*E*). In contrast, in *unc-7* mutants, some NMJs contain an enlarged single active zone region or multiple active zone regions in the same synapse (Fig. 2*B*,*F*), whereas some other synapses contain active zone regions with less differentiated structural features such as the density (Fig. 2*C*,*F*). Consistently, the distribution of active zone volumes showed a significantly increased variation in *unc-7* mutants when compared with wild-type animals for both GABAergic and cholinergic NMJs (Fig. 2*D*). These data thus confirm that *unc-7* mutants have a specific defect in active zone differentiation and/or distribution.

Proper synaptic transmission requires *unc-7*

The defects in the active zones of *unc-7* mutants suggest that presynaptic release may also be affected. We examined the efficacy of synaptic transmission in *unc-7* mutants by assaying for aldicarb resistance. Aldicarb is an acetylcholinesterase inhibitor that prevents the removal of acetylcholine from synaptic clefts. Excessive cholinergic activation leads to hypercontraction and lethality in *C. elegans*; consequently, mutants with reduced synaptic transmission confer stronger resistance to aldicarb than wild-type animals (Nguyen et al., 1995). Both *unc-7(hp121)* and *unc-7(e5)* mutants were aldicarb resistant (Fig. 3*A*) (Materials and Methods). Expression of the *unc-7* genomic clone that rescued behavior and GFP::SYD-2 defects in *unc-7(hp121)* mutants also restored aldicarb sensitivity (Fig. 3*A*), suggesting that *unc-7* mutants have a deficit in synaptic transmission.

unc-7 is required during synaptogenesis for presynaptic differentiation

hs9 is a temperature-sensitive allele of *unc-7* that displays severe kinker locomotion defects at 15°C (nonpermissive temperature) and relatively normal locomotion at 22°C (permissive temperature)

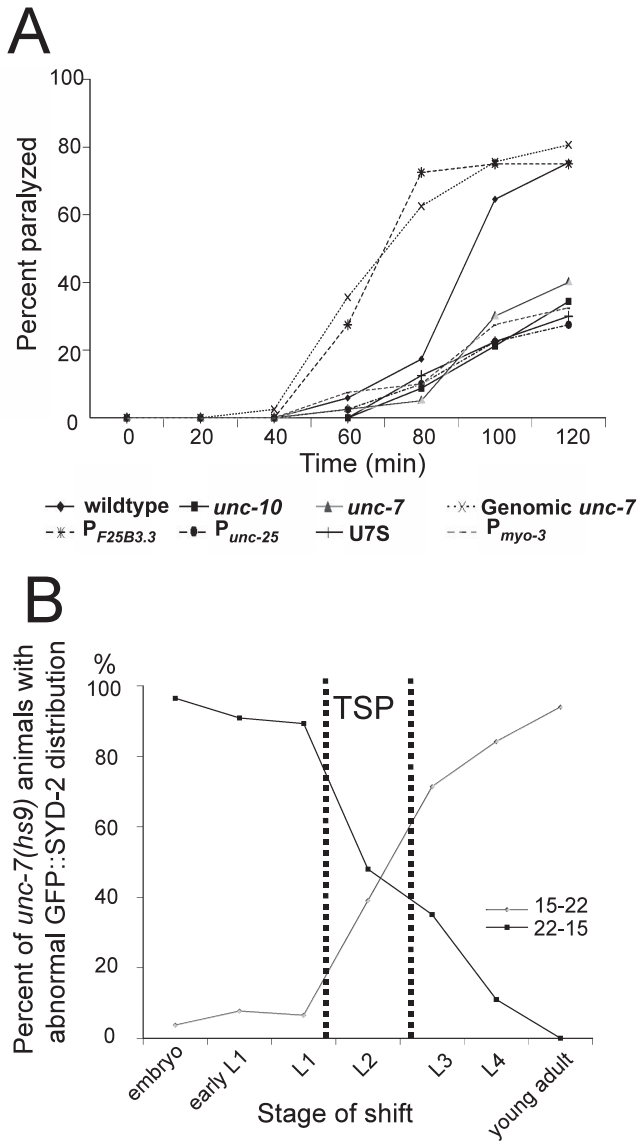

Figure 3. UNC-7 is required for both synaptic transmission and synapse formation. ***A***, *unc-7(hp121)* animals carrying a genomic *unc-7* construct and UNC-7S construct or constructs that express *unc-7* panneuronally (PF25B3.3) in muscles (P*myo-3*) or in GABAergic neurons (P*unc-25*) were assayed for aldicarb resistance. Shown here is the result of one representative set of aldicarb test result (Materials and Method). ***B***, *unc-7* is required for proper GFP::SYD-2(*hpIs3*) active zone marker morphology during a developmental stage coinciding with synaptogenesis. The percentage of adult *unc-7(hs9)* temperature-sensitive mutants showing the GFP::SYD-2 morphology defects when shifted between permissive and nonpermissive temperatures during different developmental stages. 22-15, *unc-7(hs9)* cold-sensitive mutants were shifted from 22°C (the permissive temperature) to 15°C (the nonpermissive temperature) at developmental stages indicated along the *x*-axis. Vice versa for 15–22°.

(Hecht et al., 1996). We found that *hpIs3*(GFP::SYD-2)*unc-7(hs9)* animals also displayed a temperature-dependent penentrance of active zone defects. When cultured at 15°C throughout development, 95% of the animals displayed a reduction of bright *hpIs3*(GFP::SYD-2) puncta, compared with 5% animals maintained at 22°C, consistent with UNC-7(*hs9*) function subject to temperature changes. By shifting *hpIs3*(GFP::SYD-2) *unc-7(hs9)* animals between the permissive (22°C) at nonpermissive temperature (15°C) at different developmental stages, we determined the temperature-sensitive period (TSP) for active zone formation in DD class motoneurons.

The most critical period for *unc-7(hs9)* animals to display normal GFP::SYD-2 morphology is during the late L1 to early L3 larval stages of development (Fig. 3*B*). Chemical synapses in DD neurons that persist into adulthood are formed during this stage (Walthall et al., 1993). Such a temperature-sensitive period also coincides with the developmental regulation of *unc-7* transcription, where the *unc-7* transcript level displays a sharp increase at onset of L1 and a sharp decrease by the L4 stage (Starich et al., 1993). Therefore, UNC-7 function in active zone differentiation is required at a developmental stage coinciding with the period of major synaptogenesis.

UNC-7 concentrates at specific subcellular regions in the nervous system and muscles

Whole-mount immunofluorescent staining of wild-type animals with an antibody against UNC-7 (a generous gift from Starich and Shaw) revealed specific staining in both the nervous system and muscle (Fig. 4*A–E*). This immuno-reactivity was completely absent in both *unc-7(e5)* and *unc-7(hp121)* mutants (data not shown). Along the processes of dorsal and ventral nerve cords, UNC-7 localizes to many small discrete puncta interspersed by infrequent larger puncta (Fig. 4*B*,*C*). Antibody staining against UNC-7 in a strain expressing a postsynaptic GABA receptor marker, UNC-49::GFP (*oxIs22*), further confirmed that UNC-7 puncta is present along nerve processes apposed to muscle (Fig. 4*H*). UNC-7 also localizes to discrete puncta outlining the surface of body-wall muscles, mostly at posterior muscles, and along muscle arms that extend perpendicular from toward the nerve cords (Fig. 4*D*; supplemental Fig. S2*A*, available at www.jneurosci.org as supplemental material).

The punctate immunostaining pattern of UNC-7 suggested that it is concentrated at specific subcellular regions in neurons. Previous electron microscopic reconstruction of the adult *C. elegans* nervous system revealed the presence of gap junctions mainly between neurons or between muscles. The number, distribution, and morphology of the large, periodic neuronal UNC-7 puncta resembled the description of motoneuron gap junctions. However, the numerous discrete smaller UNC-7 puncta are present along dorsal and ventral nerve processes where gap junction structures have not been described in adults (White, 1986). The punctate nature and distribution of UNC-7 along these regions suggested presynaptic localization.

To further investigate the subcellular localization of these UNC-7 puncta in neurons, we performed double immunolabeling with various presynaptic markers. Endogenous UNC-7 did not colocalize with active zone proteins UNC-10 and SYD-2 (Fig. 4*F*,*G* series). We also did not observe colocalization between UNC-7 and presynaptic GFP markers, GFP::SYD-2 or SNB-1::GFP, expressed in GABAergic neurons (Fig. 4*I*,*J* series). Instead, many UNC-7 puncta are perisynaptic, closely flanking presynaptic markers. Also, UNC-7 puncta were not directly apposed to postsynaptic UNC-49::GFP puncta (Fig. 4*H*) but appeared perisynaptic, further suggesting that the many small UNC-7 puncta flank presynaptic regions.

Since UNC-7 expression may not be limited to a single class of motoneurons in the dorsal cord, it is possible that the apparent localization of small UNC-7 puncta was attributable to the expression and localization of UNC-7 in one class of neurons next to the synapse of another class. To test this possibility, we coexpressed a GFP::UNC-7 fusion protein with presynaptic SNB-1::mRFP in GABAergic motoneurons and observed many GFP::UNC-7 puncta flanking SNB-1::mRFP (Fig. 4*K*). Therefore, we consider most UNC-7 proteins localize to additional subcellular regions distinct from presumptive gap junctions,

along the nerve processes, including regions flanking chemical synapses.

UNC-7 regulates active zone differentiation cell autonomously in motoneurons neurons

To determine in which tissue UNC-7 is required for proper active zone differentiation, we expressed *unc-7* cDNA in either neurons or muscles alone and assayed the ability to rescue the Unc behavior and the reduction in GFP::SYD-2(*hpIs3*) puncta observed in *unc-7(hp121)* mutants. Panneuronal expression of *unc-7* using the *F25B3.3 (rgef-1)* promoter (D. Pilgrim, personal communication) rescued the locomotion and defects in GABAergic active zone marker GFP::SYD-2(*hpIs3*) as well as cholinergic active zone marker GFP::SYD-2 (*hpIs54*) (Fig. 1*C–F*; supplemental Movie S5, available at www.jneurosci.org as supplemental material). In contrast, muscle expression of *unc-7* using the *myo-3* promoter rescued neither behavior nor the active zone marker defects (Fig. 1*F*; supplemental Movie S6, available at www.jneurosci.org as supplemental material) (data not shown). We also performed RNA interference (RNAi) knockdown of *unc-7*. As the *C. elegans* nervous system is refractory to RNAi (Simmer et al., 2002), many animals treated with *unc-7* RNAi showed abolished UNC-7 expression in muscles, whereas neuronal UNC-7 was unaffected (as observed by antibody staining; data not shown). We did not observe any defects in locomotion or active zone marker expression in these animals (data not shown). We thus conclude that UNC-7 is required in the nervous system for both normal locomotion and presynaptic differentiation.

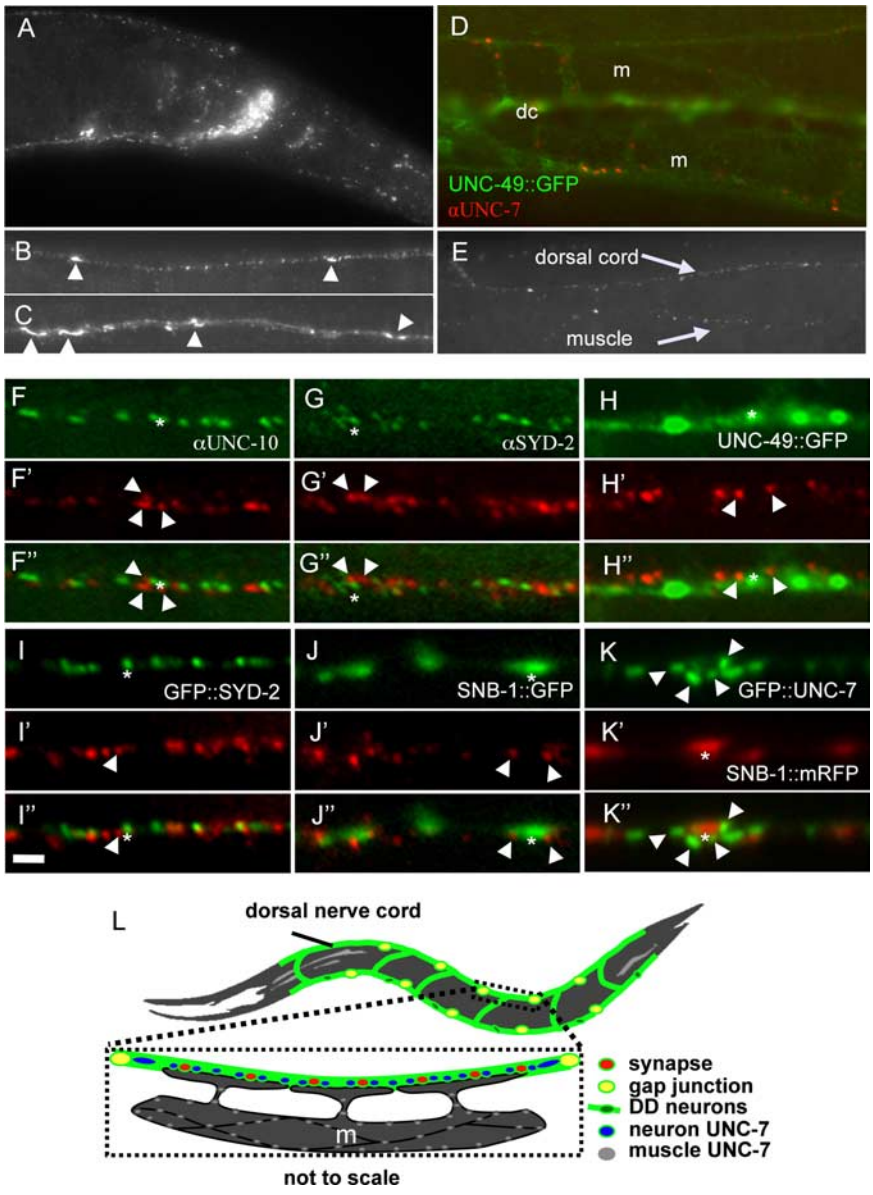

Figure 4. UNC-7 localizes to perisynaptic regions along the dorsal nerve cord and the expression of UNC-7 in neurons is required for active zone differentiation. Specific UNC-7 antibody staining in nervous system (***A***), dorsal nerve cord (***B***), ventral nerve cord (***C***), and muscle (***D***; M, muscle; dc, dorsal cord). UNC-7 staining shows small discrete puncta, as well as to larger puncta occurring periodically along nerve cords (arrowheads). ***E***, Staining of UNC-7 shows discrete puncta along the dorsal cord in the muscle. ***F–J***, Coimmunostaining of UNC-7 (red) with presynaptic proteins (green) UNC-10 (***F–F″***), SYD-2 (***G–G″***), synaptic GFP markers UNC-49::GFP (***H–H″***), SYD-2::GFP (***I–I″***), and SNB-1::GFP (***J–J″***). ***K–K″***, Live imaging of GFP::UNC-7 (green) and SNB-1::mRFP (red) in GABAergic neurons. Scale bar, 5 μm. ***L***, An illustration of UNC-7 protein localization in neurons and muscles.

We further examined if the expression of *unc-7* in GABAergic neurons was sufficient to rescue the GABAergic GFP::SYD-2(*hpIs3*) defects. Driven by the *unc-25* promoter (P*unc-25*), GABAergic expression of *unc-7* alone rescued the GABAergic GFP::SYD-2(*hpIs3*) puncta number in *unc-7(hp121)* to wild-type levels (Fig. 1*F*). GABAergic expression, however, was not sufficient to rescue the locomotion defects (supplemental Movie S7, available at www.jneurosci.org as supplemental material). Cholinergic expression of *unc-7* using the *acr-2* promoter (P*acr*-2) did not rescue behavior or GFP::SYD-2(*hpIs3*) defects (Fig. 1*F*; supplemental Movie S8, available at www.jneurosci.org as supplemental material). Similarly, cholinergic, but not GABAergic, expression of *unc-7* rescued the active zone marker defects in cholinergic GFP::SYD-2(*hpIs54*) (data not shown). All transgenic lines were verified for proper tissue-specific expression by UNC-7 immunostaining (supplemental Fig. S2, available at www.jneurosci.org as supplemental material).

A truncated version of the *unc-7* locus expresses a UNC-7 isoform, UNC-7S, specifically in interneurons, and rescued forward but not backward locomotion defects (supplemental Movie S9, available at www.jneurosci.org as supplemental material) (T. Starich and J. Shaw, unpublished observations). Interneuron driven UNC-7S expression, however, did not rescue GABAergic GFP::SYD-2(*hpIs3*) defects (Fig. 1*F*). These data indicate that, at least in motoneurons, *unc-7* is required cell autonomously for proper presynaptic differentiation and that abnormal kinker behavior is likely the total output of defects in several types of neurons.

The above constructs were also examined for their ability to restore the deficit in synaptic function assayed by aldicarb sensitivity. Panneuronal expression of *unc-7* or expression from the *unc-7* genomic construct rescued the aldicarb resistance of *unc-7(hp121)* animals (Fig. 3*A*). Muscle expression of *unc-7* did not

rescue aldicarb resistance. In addition, GABAergic expression or interneuron expression of the UNC-7S isoform did not rescue aldicarb resistance (Fig. 3*A*). Despite showing consistent and appropriate expression (supplemental Fig. S2, available at www.jneurosci.org as supplemental material), the aldicarb response of *unc-7(hp121)* animals expressing P*acr-2* driven *unc-7* did not rescue the aldicarb resistance either (data not shown). This suggests that behavioral deficits of *unc-7* mutants are contributed by, but not solely dependent on, the presynaptic differentiation and function defects revealed in motoneurons.

Perisynaptic UNC-7 is required to regulate presynaptic differentiation in GABAergic neurons

The tissue-specific expression experiments demonstrate that UNC-7 is only required in GABAergic neurons for active zone differentiation at GABAergic neuromuscular junctions. GABAergic neurons form gap junctions between neurite endings of neighboring neurons of the same class (White, 1986) (also illustrated in Fig. 4*L*). Since neuronal UNC-7 may be present at both the junctions and nonjunctional regions, we performed a mosaic analysis to determine where UNC-7 is required for active zone differentiation. We generated a strain carrying an extrachromosomal array consisting of P*unc-25*-RFP and P*unc-25-unc-7* in an *hpIs3 unc-7(hp121)* null mutant background so only GABAergic neurons express the UNC-7 protein. With the UNC-7-expressing extrachromosomal array subject to random loss during somatic cell division, mosaic animals expressing (+) or not expressing (−) UNC-7 in individual DD motoneurons were identified by RFP expression in corresponding cell bodies. With gap junction formation interrupted between DD1 UNC-7(+) and a neighboring DD2 UNC-7(−), we quantified the number of *hpIs3* puncta in the isolated DD1 neurons in L4 stage mosaic animals (supplemental Fig. S3, available at www.jneurosci.org as supplemental material).

Wild-type animals display an average of 59.7 ± 7.6 bright *hpIs3* puncta ($N = 11$) in DD1 neurons, whereas *unc-7(hp121)* animals show an ~20% reduction in bright *hpIs3* puncta (47.8 ± 5.7, $N = 14$; $p < 0.0001$ vs wild type). In *unc-7(hp121)* mosaic animals with an isolated DD1 UNC-7(+), the average number of bright GFP::SYD-2(*hpIs3*) puncta was rescued to wild-type levels (63.3 ± 8.2, $N = 7$; $p < 0.0001$ vs *hp121*), suggesting that UNC-7 is required for rescuing the active zone defects.

A possibility remained that in the above mosaic animals, DD1 UNC-7(−) neurons maintained gap junction connections with their neighbors using another innexin(s). To address this possibility, we quantified the number of bright GFP::SYD-2(*hpIs3*) puncta in mosaic animals that were DD1 UNC-7(−) but DD2 UNC-7(+). If gap junctions between them persist and are responsible for active zone differentiation, we expect a rescue of the bright GFP::SYD-2(*hpIs3*) puncta number in DD1 neurons. This is not the case, as we observed the same level of reduction in bright GFP::SYD-2(*hpIs3*) puncta number in these mosaic animals as in *unc-7(hp121)* mutants (46.1 ± 6.0, $N = 7$; $p < 0.001$ vs wild type). These results thus strongly suggest that cell-autonomous UNC-7, not neuronal coupling via UNC-7, is required for active zone differentiation.

The lack of UNC-7-dependent transient gap junctions in the anterior nerve cords of an L1 larva

The number of UNC-7 puncta in mature motor neurons is much larger than the number of gap junctions in adult animals. However, transient gap junctions are known to regulate neural development and circuit maturation, so it is possible that UNC-7 forms gap junctions early in development to promote synaptogenesis and that the UNC-7 staining along the neurites in the adult motoneurons represents the "footprints" of these transient gap junctions. To examine this possibility, we performed ultrastructural analyses of the anterior ventral and dorsal nerve cords of an early wild-type L1 larva, the earliest developmental stage with abundant *unc-7* transcription (Starich et al., 1993). The animals were sectioned at a time corresponding to the onset of chemical synaptogenesis in motoneurons and at the beginning of the critically required *unc-7* TSP period for proper active zone marker expression.

Examination of this L1 larva provided no evidence for exuberant early gap junctions in the most anterior nerve cords. Five gap junction-like structures were evident in a total number of 90 sections, a 4.5 μm distance encompassing ~10 chemical synapses. Two of these gap junctions were found between an axon and a muscle arm (Fig. 5*A*, arrow) and three were found at the junction of two axons (Fig. 5*B*, arrow). This small number of gap junctions does not correspond to the dense UNC-7 expression pattern. We did note the frequent presence of "junctional" structures of a previously undescribed morphology between axons and between axon and muscles (Fig. 5*A*,*B*′, asterisks). These structures were less dense than gap junctions; they were rarely present by traditional chemical fixation but were frequently detectable by high-pressure freezing fixation (our unpublished observations). The unknown structural features were also observed frequently in the adult nervous systems of wild-type (Fig. 5*C*, asterisks) and *unc-7(hp121)* animals (Fig. 5*D*, asterisks), so they are unlikely to be *unc-7*-dependent. Thus, these results failed to demonstrate a high frequency of L1 gap junctions associated with nascent synapses.

Another innexin, UNC-9, functions identically to UNC-7 in regulating locomotion and active zone differentiation

Of the 25 innexins in *C. elegans*, only a few have been reported to express in the nervous system and even fewer in the motoneurons (Phelan and Starich, 2001; Sieburth et al., 2005). Among them, UNC-9 shows the highest amino acid sequence homology to UNC-7, and *unc-9* mutants share identical, kinker locomotion deficits with *unc-7* mutants (Barnes and Hekimi, 1997). Furthermore, *unc-9(fc16)unc-7(e5)* double-null mutants behave like either single mutant (supplemental Movie S11, available at www.jneurosci.org as supplemental material), suggesting that *unc-9* functions in the same pathway as *unc-7*.

We analyzed the synaptic morphology and function in *unc-9* mutants. *unc-9* mutants (*e101* and *fc16*) displayed a GFP::SYD-2(*hpIs3*) and GFP::UNC-10(*hpIs61*) phenotype that was similar to *unc-7* mutants (Fig. 6*A–F*) (data not shown). Quantification of GFP::SYD-2(*hpIs3*) puncta in the DD5 motoneuron of *unc-9(fc16)* null mutants revealed a reduction of the bright puncta similar to *unc-7* mutants (Fig. 6*I*). Also as in *unc-7* mutants, the other active zone marker GFP::UNC-10(*hpIs61*) was also uneven in size in *unc-9(fc16)* mutant (Fig. 6*E*,*F*), with larger variation in the puncta width ($p < 10^{-10}$ vs wild type) (Fig. 6*K*). The identical GFP::UNC-10(*hpIs61*) marker defect was observed in another kinker mutant *unc-1* (Fig. 6*H*), which was recently shown to function with UNC-9 (Chen et al., 2007). The vesicle marker *juIs1* appeared normal in morphology as well as the total number (supplemental Fig. S1, available at www.jneurosci.org as supplemental material). Last, *unc-7unc-9* double mutants showed identical active zone marker defects as single mutant ($p = 0.007$ vs wild type, and $p = 0.442$ vs *unc-7*) (Fig. 6*G*). Over-expression of UNC-7 innexin in *unc-9* mutants, or

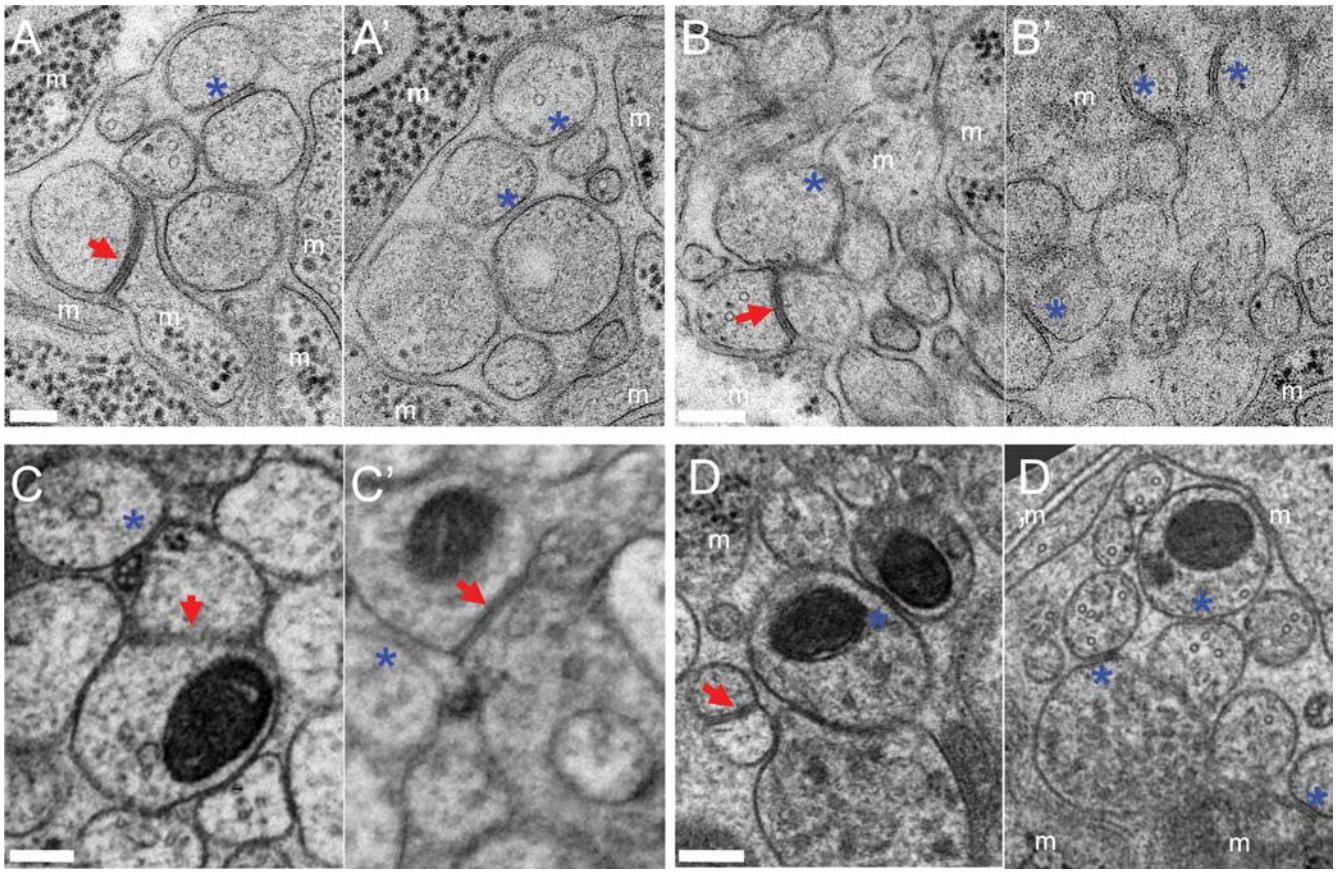

Figure 5. The presence of gap junctions at the dorsal and ventral nerve cords of wild-type and *unc-7(hp121)* animals by electron microscopy analyses. ***A–B′***, The cross sections of the dorsal (***A***, ***A′***) and ventral (***B***, ***B′***) nerve cords of a wild-type L1 larva. Circles present the cross sections of the nerve processes. m, Cross sections of the postsynaptic muscle arms that wrap around the nerve process bundles. Red arrows, Gap junctions; blue asterisks, examples of the uncharacterized "wannabe" junctions. ***C***, The cross sections of the ventral nerve cord of a wild-type adult with gap junctions shown in red arrows and wannabe junctions in blue asterisks. ***D***, The cross sections of the ventral and dorsal nerve cords of an *unc-7(hp121)* adult. Scale bars, 100 nm.

vice versa, does not rescue the defects in locomotion or active zone marker expression of the respective mutants (data not shown), consistent with *unc-9* innexin functioning in the same genetic pathway with *unc-7* to regulate active zone differentiation.

We further examined the expression pattern of UNC-9 using an UNC-9-specific antibody affinity-purified from a published reagent (Chen et al., 2007) (Materials and Methods). The further purified UNC-9 displays punctate patterns in muscles and neurons that are highly reminiscent to that of UNC-7. Similar to UNC-7, along the nerve cords, UNC-9 is also present as sparse large puncta, interspersed by numerous small puncta (data not shown). Last, UNC-9 and UNC-7::GFP puncta display almost complete colocalization in neurons and muscles (Fig. 6*J*). Thus, *unc-9* behaves similarly to *unc-7* with respect to active zone defects, as well as subcellular localization, suggesting that they function in a similar manner in active zone differentiation.

Discussion

UNC-7 innexin may have a direct role in active zone differentiation

In this study, we revealed an unexpected role for two *C. elegans* innexins, UNC-7 and UNC-9, in regulating active zone differentiation. Mutants in these proteins lead to abnormal sizes and distribution of active zones. The temporal requirement for UNC-7 is near the time of synaptogenesis. In addition to localizing to presumptive gap junctional regions, UNC-7 proteins also localize around active zones, at perisynaptic regions, at and after a developmental window for synaptogenesis. We suggest that UNC-7 proteins may form a structural corral that helps the incorporation and distribution of active zone components in a discrete region.

There are alternative models in which UNC-7 forms gap junctions, which indirectly affect chemical synapse formations. First, there might be an activity-dependent role of gap junctional coupling that affects chemical synapses. Second, there could be transient gap junctions early in development that were not observed in our electron microscopy (EM) analyses; such structures have been observed in many developing nervous systems, including that of *C. elegans* (Saint-Amant and Drapeau, 2001; Hestrin and Galarreta, 2005; Chuang et al., 2007).

An argument against these models is the strictly cell-autonomous requirement for UNC-7 in neurons whose active zones are affected. All models in which UNC-7 functions as a gap junction, whether homomeric or heteromeric during active zone differentiation, predict a degree of nonautonomous effects of its expression in a surrounding cell. This nonautonomy was first rigorously excluded for muscle, the target of most GABAgic synapses: expression of UNC-7 in muscle is neither necessary nor sufficient for an effect on active zones of GABAergic NMJs.

The mosaic analyses further demonstrated that when UNC-7 was present in a single motoneuron, while all surrounding cells were devoid of UNC-7, it was sufficient to restore normal active zone marker expression in this neuron alone. Conversely, when UNC-7 was absent from a single neuron when the neighboring

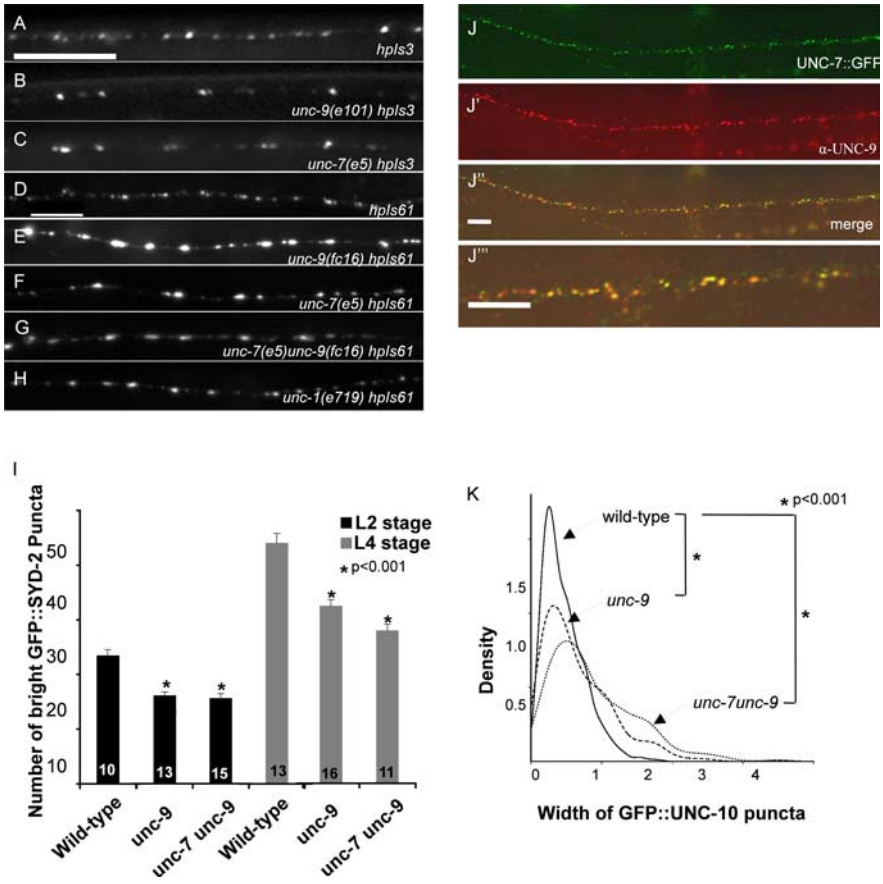

Figure 6. UNC-9 innexin functions similarly to UNC-7 during active zone differentiation. ***A–C***, GABAergic active zone marker GFP::SYD-2 expression in wild-type (*hpls3*), *unc-9(e101)*, and *unc-7(e5)* animals. ***D–H***, Active zone marker GFP::UNC-10 expression in wild-type (*hpls61*), *unc-9(fc16)*, *unc-7(e5)*, *unc-7(e5)unc-9(fc16)*, and *unc-1(e719)* animals. ***I***, Quantification of bright *hpls3* puncta in DD5 motoneurons of L2 and L4 larvae. The number of animals analyzed is shown in each bar graph. ***J–J‴***, Coimmunostaining of anti-UNC-9 and anti-GFP antibody in UNC-7::GFP expressing animals showed colocalization between UNC-9 and UNC-7::GFP. ***J‴*** provides an enlarged view of ***J′***. ***K***, The distribution curve of the GFP::UNC-10(*hpls61*) punctum width (*x*-axis in micrometers) in L3 larvae of wild-type (solid line), *unc-9(fc16)*, and *unc-7(e5)unc-9(fc16)* (dotted line) animals. *N* (the total number of puncta) = 577 (wild type), 378 (*unc-9*), and 237 (*unc-7unc-9*). Scale bars: ***A*** (for ***A–C***), ***D*** (for ***D–H***), ***J′*** (for ***J–J′***), ***J‴***, 5 μm.

neurons were UNC-7 positive, this neuron remained to be defective for the active zone marker expression. In contrast, NSY-5, a *C. elegans* innexin that does form transient gap junctions in development, has abundant nonautonomous effects (Chuang et al., 2007). Our current ultrastructural evidence also appears to be consistent with the genetic evidence.

The alternative models of UNC-7 regulating active zone differentiation through gap junction activities, however, are not entirely excluded; the EM analyses are limited by the small sample size and isolated time points during development. Our studies do not exclude an additional role of UNC-7 and UNC-9 in gap junction formation either. The localization of UNC-7 and UNC-9 to regions that do resemble gap junctions supports the contribution of these innexins for cell coupling in many aspects of development. For example, UNC-9 also mediates the electric coupling of body-wall muscles (Liu et al., 2006).

UNC-7 and UNC-9 may form hemichannels or adhesive complexes at perisynaptic regions

In addition to presumptive gap junction localizations, UNC-7 protein has a perisynaptic localization throughout development and is tightly localized with a second innexin protein, UNC-9. However, consistent with previous ultrastructural analysis (White, 1986), characteristic gap junction structures were not present within 560 nm flanking active zones of the synapses we analyzed. Therefore, UNC-7/UNC-9 may have an alternative function, acting either as hemichannels, or as adhesive proteins, in addition to gap junctions.

Hemichannels are protein complexes made of gap junction components that can open directly into the extracellular milieu to control the flux of ions and/or signaling molecules. The presence and function of physiologically relevant hemichannels has been the subject of debate. In heterologous cell expression systems, passage of currents and small molecules can be detected from connexin-type hemichannels; however, these are usually under atypical physiological conditions of very low calcium (Contreras et al., 2003; De Vuyst et al., 2006). Pannexins have recently emerged as strong candidates for *in vivo* hemichannel activities (Pelegrin and Surprenant, 2006; Thompson et al., 2006, 2008). Despite the presence of >30 invertebrate innexins, only three innexins, including *Drosophila* Shaking-B and *C. elegans* INX-3 and NSY-5 have been reported to form functional gap junctions in *Xenopus* oocytes (Phelan et al., 1998; Landesman et al., 1999; Chuang et al., 2007). Interestingly, the localization of UNC-7 protein resembles the localization of the novel channel type/putative nematode calcium channel (NCA)/UNC-77 leak channels, and the distribution of active zones in *unc-7* mutants resembles that of *nca(gf)* mutants (Yeh et al., 2008) (supplemental Fig. S4, available at www.jneurosci.org as supplemental material). Perhaps the UNC-7 channel and the NCA channel modulate each other's localization or activity.

Another possible role for innexins is as adhesion proteins to influence the incorporation of active zones along axons. Connexins have been shown to have adhesive roles in migrating cells, independent of their ability to pass current in gap junctions (Xu et al., 2006; Elias et al., 2007). Distinguishing between these models will require future structure–function analyses that are currently lacking for innexins and pannexins.

Pannexin/innexin family proteins may regulate active zone formation

Our understanding of the regulatory mechanisms involved in active zone formation remains limited. We unexpectedly revealed the direct involvement of innexins UNC-7 and UNC-9 in chemical synaptogenesis. Our results are consistent with a nonjunctional role for innexins during chemical synapse formation, but alternative mechanisms cannot be completely excluded. Further molecular and genetic studies will provide details into the mechanism through which active zone formation is regulated.

Pannexins, related mammalian homologs, are expressed abundantly in the CNS. Pannexins can form nonjunctional

hemichannels that are functionally distinct from connexin hemichannels in heterologous cells and in cultured neurons, raising the prospect that pannexins may possess unique, currently unknown physiological functions in the nervous system. The contribution of the pannexin-1-mediated hemichannel activity under ischemic condition, or during the epileptic form seizure activity, has been reported in cultured neurons or brain slices recently (Thompson et al., 2006, 2008). Whether the role of UNC-7 and UNC-9 in chemical synaptogenesis is evolutionarily conserved by pannexins awaits investigation.

References

Barnes TM, Hekimi S (1997) The *C. elegans* avermectin resistance and anesthetic response gene *unc-9* encodes a member of a protein family implicated in electrical coupling of excitable cells. J Neurochem 69:2251–2260.

Bennett MV, Zukin RS (2004) Electrical coupling and neuronal synchronization in the Mammalian brain. Neuron 41:495–511.

Brenner S (1974) The genetics of *C. elegans.* Genetics 77:71–94.

Bruzzone R, Hormuzdi SG, Barbe MT, Herb A, Monyer H (2003) Pannexins, a family of gap junction proteins expressed in brain. Proc Natl Acad Sci U S A 100:13644–13649.

Chen B, Liu Q, Ge Q, Xie J, Wang ZW (2007) UNC-1 regulates gap junctions important to locomotion in *C. elegans.* Curr Biol 17:1334–1339.

Chuang CF, Vanhoven MK, Fetter RD, Verselis VK, Bargmann CI (2007) An innexin-dependent cell network establishes left-right neuronal asymmetry in *C. elegans.* Cell 129:787–799.

Connors BW, Long MA (2004) Electrical synapses in the mammalian brain. Annu Rev Neurosci 27:393–418.

Contreras JE, Sáez JC, Bukauskas FF, Bennett MV (2003) Gating and regulation of connexin 43 (Cx43) hemichannels. Proc Natl Acad Sci U S A 100:11388–11393.

Couteaux R, Pécot-Dechavassine M (1970) [Synaptic vesicles and pouches at the level of "active zones" of the neuromuscular junction]. C R Acad Sci Hebd Seances Acad Sci D 271:2346–2349.

De Vuyst E, Decrock E, Cabooter L, Dubyak GR, Naus CC, Evans WH, Leybaert L (2006) Intracellular calcium changes trigger connexin 32 hemichannel opening. EMBO J 25:34–44.

Dvoriantchikova G, Ivanov D, Panchin Y, Shestopalov VI (2006) Expression of pannexin family of proteins in the retina. FEBS Lett 580:2178–2182.

Elias LA, Wang DD, Kriegstein AR (2007) Gap junction adhesion is necessary for radial migration in the neocortex. Nature 448:901–907.

Hecht RM, Norman MA, Vu T, Jones W (1996) A novel set of uncoordinated mutants in *C. elegans* uncovered by cold-sensitive mutations. Genome 39:459–464.

Hestrin S, Galarreta M (2005) Electrical synapses define networks of neocortical GABAergic neurons. Trends Neurosci 28:304–309.

Höfer T, Venance L, Giaume C (2002) Control and plasticity of intercellular calcium waves in astrocytes: a modeling approach. J Neurosci 22:4850–4859.

Hung W, Hwang C, Po MD, Zhen M (2007) Neuronal polarity is regulated by a direct interaction between a scaffolding protein, Neurabin, and a presynaptic SAD-1 kinase in *C. elegans*. Development 134:237–249.

Kim JS, Lilley BN, Zhang C, Shokat KM, Sanes JR, Zhen M (2008) A chemical-genetic strategy reveals distinct temporal requirements for SAD-1 kinase in neuronal polarization and synapse formation. Neural Dev 3:23.

Koushika SP, Richmond JE, Hadwiger G, Weimer RM, Jorgensen EM, Nonet ML (2001) A post-docking role for active zone protein Rim. Nat Neurosci 4:997–1005.

Krishnan SN, Frei E, Swain GP, Wyman RJ (1993) Passover: a gene required for synaptic connectivity in the giant fiber system of *Drosophila*. Cell 73:967–977.

Kumar NM, Gilula NB (1996) The gap junction communication channel. Cell 84:381–388.

Landesman Y, White TW, Starich TA, Shaw JE, Goodenough DA, Paul DL (1999) Innexin-3 forms connexin-like intercellular channels. J Cell Sci 112:2391–2396.

Li S, Dent JA, Roy R (2003) Regulation of intermuscular electrical coupling by the *C. elegans* innexin inx-6. Mol Biol Cell 14:2630–2644.

Liu Q, Chen B, Gaier E, Joshi J, Wang ZW (2006) Low conductance gap junctions mediate specific electrical coupling in body-wall muscle cells of *C. elegans.* J Biol Chem 281:7881–7889.

Locovei S, Bao L, Dahl G (2006) Pannexin 1 in erythrocytes: function without a gap. Proc Natl Acad Sci U S A 103:7655–7659.

Nguyen M, Alfonso A, Johnson CD, Rand JB (1995) *C. elegans* mutants resistant to inhibitors of acetylcholinesterase. Genetics 140:527–535.

Nonet ML (1999) Visualization of synaptic specializations in live *C. elegans* with synaptic vesicle protein-GFP fusions. J Neurosci Methods 89:33–40.

Pelegrin P, Surprenant A (2006) Pannexin-1 mediates large pore formation and interleukin-1beta release by the ATP-gated P2X7 receptor. EMBO J 25:5071–5082.

Personius KE, Balice-Gordon RJ (2002) Activity-dependent synaptic plasticity: insights from neuromuscular junctions. Neuroscientist 8:414–422.

Peters MA, Teramoto T, White JQ, Iwasaki K, Jorgensen EM (2007) A calcium wave mediated by gap junctions coordinates a rhythmic behavior in *C. elegans.* Curr Biol 17:1601–1608.

Phelan P, Starich TA (2001) Innexins get into the gap. Bioessays 23:388–396.

Phelan P, Stebbings LA, Baines RA, Bacon JP, Davies JA, Ford C (1998) *Drosophila* Shaking-B protein forms gap junctions in paired *Xenopus* oocytes. Nature 391:181–184.

Phelan P, Goulding LA, Tam JL, Allen MJ, Dawber RJ, Davies JA, Bacon JP (2008) Molecular mechanism of rectification at identified electrical synapses in the *Drosophila* giant fiber system. Curr Biol 18:1955–1960.

Revel JP, Karnovsky MJ (1967) Hexagonal array of subunits in intercellular junctions of the mouse heart and liver. J Cell Biol 33:C7–C12.

Romanov RA, Rogachevskaja OA, Bystrova MF, Jiang P, Margolskee RF, Kolesnikov SS (2007) Afferent neurotransmission mediated by hemichannels in mammalian taste cells. EMBO J 26:657–667.

Rostaing P, Weimer RM, Jorgensen EM, Triller A, Bessereau JL (2004) Preservation of immunoreactivity and fine structure of adult *C. elegans* tissues using high-pressure freezing. J Histochem Cytochem 52:1–12.

Saint-Amant L, Drapeau P (2001) Synchronization of an embryonic network of identified spinal interneurons solely by electrical coupling. Neuron 31:1035–1046.

Sieburth D, Ch'ng Q, Dybbs M, Tavazoie M, Kennedy S, Wang D, Dupuy D, Rual JF, Hill DE, Vidal M, Ruvkun G, Kaplan JM (2005) Systematic analysis of genes required for synapse structure and function. Nature 436:510–517.

Simmer F, Tijsterman M, Parrish S, Koushika SP, Nonet ML, Fire A, Ahringer J, Plasterk RH (2002) Loss of the putative RNA-directed RNA polymerase RRF-3 makes *C. elegans* hypersensitive to RNAi. Curr Biol 12:1317–1319.

Söhl G, Maxeiner S, Willecke K (2005) Expression and functions of neuronal gap junctions. Nat Rev Neurosci 6:191–200.

Starich TA, Herman RK, Shaw JE (1993) Molecular and genetic analysis of unc-7, a *C. elegans* gene required for coordinated locomotion. Genetics 133:527–541.

Sulston JE, Horvitz HR (1977) Post-embryonic cell lineages of the nematode, *C. elegans*. Dev Biol 56:110–156.

Thompson RJ, Zhou N, MacVicar BA (2006) Ischemia opens neuronal gap junction hemichannels. Science 312:924–927.

Thompson RJ, Jackson MF, Olah ME, Rungta RL, Hines DJ, Beazely MA, MacDonald JF, MacVicar BA (2008) Activation of pannexin-1 hemichannels augments aberrant bursting in the hippocampus. Science 322:1555–1559.

Vanden Abeele F, Bidaux G, Gordienko D, Beck B, Panchin YV, Baranova AV, Ivanov DV, Skryma R, Prevarskaya N (2006) Functional implications of calcium permeability of the channel formed by pannexin 1. J Cell Biol 174:535–546.

Venance L, Stella N, Glowinski J, Giaume C (1997) Mechanism involved in initiation and propagation of receptor-induced intercellular calcium signaling in cultured rat astrocytes. J Neurosci 17:1981–1992.

Vogt A, Hormuzdi SG, Monyer H (2005) Pannexin1 and Pannexin2 expression in the developing and mature rat brain. Brain Res Mol Brain Res 141:113–120.

Walthall WW, Li L, Plunkett JA, Hsu CY (1993) Changing synaptic specificities in the nervous system of *C. elegans*: differentiation of the DD motoneurons. J Neurobiol 24:1589–1599.

Wang Y, Gracheva EO, Richmond J, Kawano T, Couto JM, Calarco JA, Vijayaratnam V, Jin Y, Zhen M (2006) The C2H2 zinc-finger protein SYD-9

is a putative posttranscriptional regulator for synaptic transmission. Proc Natl Acad Sci U S A 103:10450–10455.

Watanabe T, Kankel DR (1990) Molecular cloning and analysis of l(1)ogre, a locus of *Drosophila melanogaster* with prominent effects on the postembryonic development of the central nervous system. Genetics 126:1033–1044.

White JG (1986) The structure of the nervous system of the nematode *C. elegans.* Philos Trans R Soc Lond B Biol Sci 314:1–340.

Whitten SJ, Miller MA (2007) The role of gap junctions in *C. elegans* oocyte maturation and fertilization. Dev Biol 301:432–446.

Xu X, Francis R, Wei CJ, Linask KL, Lo CW (2006) Connexin 43-mediated modulation of polarized cell movement and the directional migration of cardiac neural crest cells. Development 133:3629–3639.

Yeh E, Kawano T, Weimer RM, Bessereau JL, Zhen M (2005) Identification of genes involved in synaptogenesis using a fluorescent active zone marker in *C. elegans.* J Neurosci 25:3833–3841.

Yeh E, Ng S, Zhang M, Bouhours M, Wang Y, Wang M, Hung W, Aoyagi K, Melnik-Martinez K, Li M, Liu F, Schafer WR, Zhen M (2008) A putative cation channel, NCA-1, and a novel protein, UNC-80, transmit neuronal activity in *C. elegans*. PLoS Biol 6:e55.

Zhai RG, Bellen HJ (2004) The architecture of the active zone in the presynaptic nerve terminal. Physiology (Bethesda) 19:262–270.

Zhen M, Jin Y (1999) The liprin protein SYD-2 regulates the differentiation of presynaptic termini in *C. elegans*. Nature 401:371–375.

Zoidl G, Petrasch-Parwez E, Ray A, Meier C, Bunse S, Habbes HW, Dahl G, Dermietzel R (2007) Localization of the pannexin1 protein at postsynaptic sites in the cerebral cortex and hippocampus. Neuroscience 146:9–16.